Journal Pre-proofs

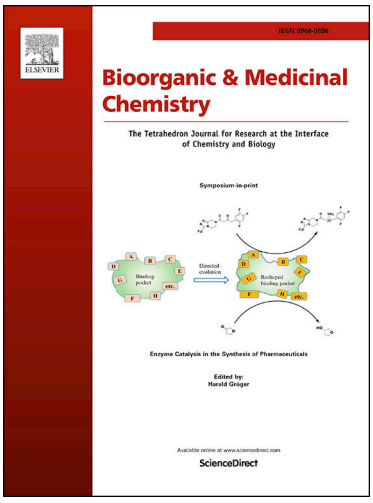

Discovery of a new potent inhibitor of mushroom tyrosinase (*Agaricus bisporus)* containing 4-(4-hydroxyphenyl)piperazin-1-yl moiety

Laura De Luca, Maria Paola Germanò, Antonella Fais, Francesca Pintus, Maria Rosa Buemi, Serena Vittorio, Salvatore Mirabile, Antonio Rapisarda, Rosaria Gitto

PII: S0968-0896(20)30318-7
DOI: https://doi.org/10.1016/j.bmc.2020.115497
Reference: BMC 115497

To appear in: *Bioorganic & Medicinal Chemistry*

Received Date: 27 November 2019
Revised Date: 16 March 2020
Accepted Date: 7 April 2020

Please cite this article as: L. De Luca, M. Paola Germanò, A. Fais, F. Pintus, M. Rosa Buemi, S. Vittorio, S. Mirabile, A. Rapisarda, R. Gitto, Discovery of a new potent inhibitor of mushroom tyrosinase (*Agaricus bisporus)* containing 4-(4-hydroxyphenyl)piperazin-1-yl moiety, *Bioorganic & Medicinal Chemistry* (2020), doi: https://doi.org/10.1016/j.bmc.2020.115497

Graphical Abstract

Discovery of a new potent inhibitor of mushroom tyrosinase (*Agaricus bisporus*) containing 4-(4-hydroxyphenyl)piperazin-1-yl moiety

Leave this area blank for abstract info.

Laura De Luca[a], Maria Paola Germanò[a], Antonella Fais[b], Francesca Pintus[b], Maria Rosa Buemi[a], Serena Vittorio[a], Salvatore Mirabile[a], Antonio Rapisarda[a] and Rosaria Gitto[a]

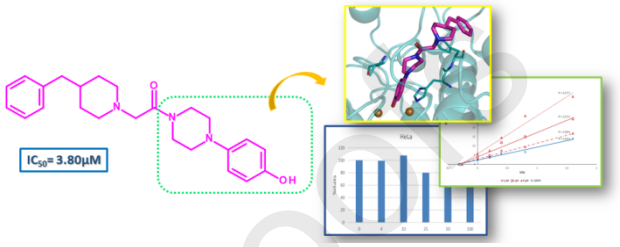

[a]*Department of Chemical, Biological, Pharmaceutical, and Environmental Sciences, Polo Universitario SS. Annunziata, University of Messina, Viale Palatucci 13, I-98168 Messina, Italy*
[b]*Department of Life and Environment Sciences, University of Cagliari, I-09042 Monserrato, Cagliari, Italy*

ELSEVIER

Bioorganic & Medicinal Chemistry
journal homepage: www.elsevier.com

Discovery of a new potent inhibitor of mushroom tyrosinase (*Agaricus bisporus)* containing 4-(4-hydroxyphenyl)piperazin-1-yl moiety

Laura De Luca[a,*], Maria Paola Germanò[a], Antonella Fais[b], Francesca Pintus[b], Maria Rosa Buemi[a], Serena Vittorio[a], Salvatore Mirabile[a], Antonio Rapisarda[a] and Rosaria Gitto[a]

[a]*Department of Chemical, Biological, Pharmaceutical, and Environmental Sciences, Polo Universitario SS. Annunziata, University of Messina, Viale Palatucci 13, I-98168 Messina, Italy*
[b]*Department of Life and Environment Sciences, University of Cagliari, I-09042 Monserrato, Cagliari, Italy*

ARTICLE INFO

Article history:
Received
Received in revised form
Accepted
Available online

Keywords:
Keyword_1 Tyrosinase inhibitors
Keyword_2 Phenylpiperazines
Keyword_3 Docking studies
Keyword_4 *Agaricus Bisporus*
Keyword_5 Hela cells

ABSTRACT

Tyrosinase (TYR, EC 1.14.18.1) plays a pivotal role in mammalian melanogenesis and enzymatic browning of plant-derived food. Therefore, tyrosinase inhibitors (TYRIs) can be of interest in cosmetics and pharmaceutical industries as depigmentation compounds as well as anti-browning agents. Starting from 4-benzylpiperidine derivatives that showed good inhibitory properties toward tyrosinase from *Agaricus bisporus* (TyM), we synthesized a new series of TYRIs named 3-(4-benzyl-1-piperidyl)-1-(4-phenylpiperazin-1-yl)propan-1-one and 2-(4-benzyl-1-piperidyl)-1-(4-phenylpiperazin-1-yl)ethanone derivatives. Among them, compound **4b** proved to be the most potent inhibitor (IC_{50}= 3.80 μM) and it also showed a good antioxidant activity. These new data furnished additional information about the SAR for this class of TYRIs.

1. Introduction

Tyrosinase (TYR, EC 1.14.18.1) is a copper-containing enzyme widely distributed in nature. It is involved in the biosynthesis of melanin, a glycoprotein that is produced in melanocytes and responsible for pigmentation of skin, hair and eyes in humans. From a structural point of view, TYR possesses three domains called central, N-terminal and C-terminal. The different TYR isoforms expressed in various organisms share the same catalytic central domain, which comprises six conserved histidine residues and the two copper ions. [1, 2] TYR catalyzes two types of oxidation reactions: *o*-hydroxylation (monophenolase activity) and *o*-oxidation (diphenolase activity) (Figure 1). [1]

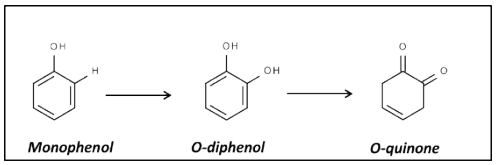

Figure 1. Schematic representation of TYR enzymatic activity

Additionally, free radicals also play an important role in the biosynthesis of melanin, and several studies have shown that free radicals are involved in the catalytic reactions of tyrosinase. Evidences have shown that for several active compounds the antioxidant activity is combined with tyrosinase inhibition.[3] Although melanin is crucial for protecting the skin from UV radiations, an abnormal melanin production can result in various skin diseases, such as skin hyper-pigmentation and melanoma. As disorders in melanogenesis seems to be linked to the neurodegenerative pathologies including Parkinson's, Alzheimer's, and Huntington's diseases, TYR inhibitors might help finding new way in the treatment of these relevant pathologies.[2]

It has been demonstrated that the competitive or noncompetitive inhibition of TYR activity is the mode of action of active molecules from synthetic and natural sources[4] such as kojic acid, [5-8], tropolone [9] but also several chalcones, flavonoids, [10,11,12] coumarins,[13] thioureas, peptides, and other heterocyclic compounds. [14-17]

In our quest to identify further chemotypes as TYR inhibitors (TYRIs) from synthetic source, we previously carried out computational studies and demonstrated that the 4-fluorobenzylpiperidine fragment exerts a crucial role during the binding of TYRIs into the enzymatic cavity. Particularly, Figure 2

A sh
dimethoxy-1H-indol-3-yl)-3-(4-(4-fluorobenzyl)piperidin-1-yl)propan-1-one **I**,[18,19] having better affinity when compared with standard compound kojic acid (KA) (IC_{50} = 7.56 µM versus IC_{50} = 17.76 µM against TyM, respectively). [20] In details, the aromatic moiety could establish favorable contacts with residues His244, His263 and Val283. These observations were confirmed by X-ray studies that revealed that the 4-fluorobenzyl fragment is located near to the two copper ions in the active site of tyrosinase from Bacillus megaterium (TyBm) (Figure 2B) that presents homology with TyM. [20]

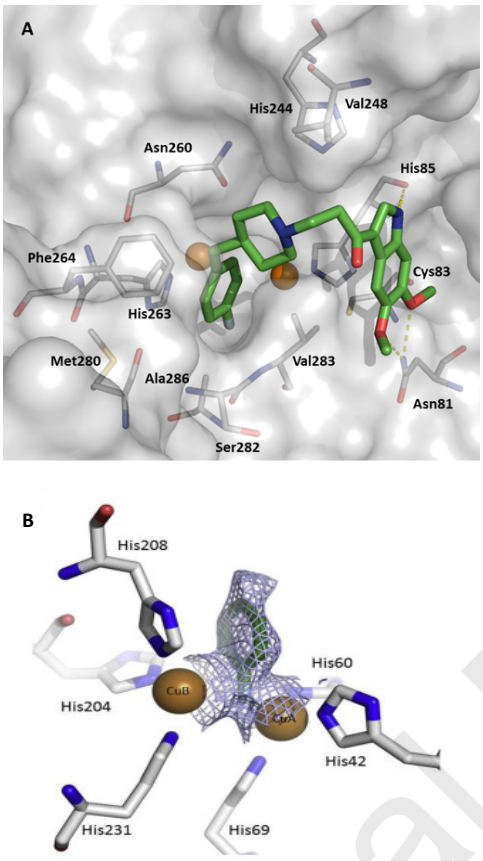

Figure 2. (A) Plausible binding mode of 1-(5,6-dimethoxy-1H-indol-3-yl)-3-(4-(4-fluorobenzyl)piperidin-1-yl)propan-1-one (**I**) docked into the catalytic site of TyM retrieved from PDB database (PDB 2Y9X). (B) Cocrystal structure of the 4-fluorobenzyl portion of prototype **I** and TyBm. [20]

Keeping in mind the significant inhibitory activity observed for prototype **I**,[20] we planned the synthesis of a new series of molecules. Particularly, we chose to maintain the benzylpiperidine fragment of prototype **I** and to modify the remaining molecular portion thus introducing a more flexible fragment in place of indole ring.

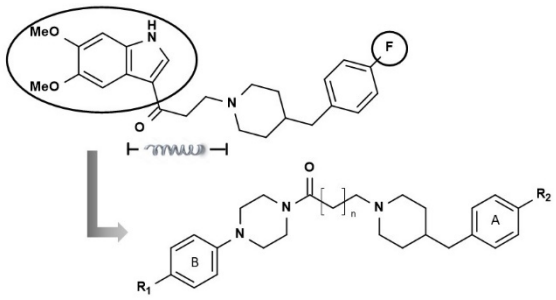

Figure 3. Chemical structure of 1-(5,6-dimethoxy-1H-indol-3-yl)-3-(4-(4-fluorobenzyl)piperidin-1-yl)propan-1-one (**I**) and designed compounds

As depicted in Figure 3 we modified the left portion as follow: (a) to ascertain the role of the presence of hydrophobic-aromatic "tail" we replaced the indole ring with an arylpiperazine fragment; (b) to verify the "optimized" distance between aromatic rings we reduced the linker between the arylpiperazine and benzylpiperidine moieties; (c) we also introduced fluorine atom as substituent (R_2) on aromatic ring (A) of benzylpiperidine and probed the influence of the introduction of hydroxyl group (R_1) on the aromatic ring (B) of phenylpiperazine.

All the designed compounds were synthesized and tested in biological assays on mushroom's tyrosinase (TyM). For selected active inhibitors we further explored antioxidant activity and cytotoxicity as well as the mechanism of action.

2. Results and Discussion

We planned the synthesis of the designed 2-(4-benzyl-1-piperidyl)-1-(4-phenylpiperazin-1-yl)ethanone derivatives **4a-b** and **5a-b** and 3-(4-benzyl-1-piperidyl)-1-(4-phenylpiperazin-1-yl)propan-1-one **6a-b** and **7a-b**, that were prepared in good yields following the synthetic route described in Scheme 1. The suitable piperazine **1a-b** were coupled with 2-chloroacetyl chloride or 3-chloropropanoyl chloride to give corresponding intermediates 2-chloro-1-(4-phenylpiperazin-1-yl)ethanones (**2a-b**) and 3-chloro-1-(4-phenylpiperazin-1-yl)propan-1-ones (**3a-b**). We began the synthesis in alkaline medium by TEA at 0°C; however, the same reaction performed at room temperature without TEA led an improvement in yields. Then, the intermediates **2a-b** and **3a-b** reacted in microwave-assisted conditions with suitable benzylpiperidine derivatives thus affording the eight designed compounds **4a-b, 5a-b, 6a-b** and **7a-b**. Analytical and spectral data of all synthesized compounds were in full agreement with the proposed structures (see Experimental part and Supporting Material).

Scheme 1

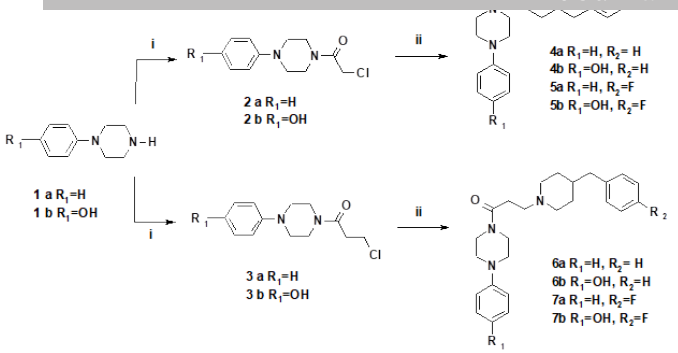

Reagents and conditions (i) 2-Chloroacetyl chloride or 3-chloropropanoyl chloride, DCM, 1h, r.t.; (ii) K_2CO_3, DMF, 15 min at 100 °C (MW)

All synthesized compounds **4a-b**, **5a-b**, **6a-b** and **7a-b** were tested as tyrosinase inhibitors using TyM. The inhibitory effects were reported in terms of diphenolase activity in Table 1, using kojic acid and prototype **I** as reference compounds.

By analyzing the data collected in the Table 1 it emerged that all tested compounds are able to inhibit TyM displaying IC_{50} values ranging from 3.80 to 80.86 µM. It is interesting to note that compounds **4b**, **5b**, **6b** and **7b** were effective inhibitors in low micromolar range. The best active inhibitors **4b** and **6b** resulted more potent than lead compound **I** (IC_{50} = 7.56 µM) and kojic acid (IC_{50} = 17.76 µM). Structure-activity relationship (SAR) analysis pointed out the relevance of fluorine and/or hydroxyl substituents on aromatic rings.

Table 1. TyM inhibitory effects of compounds **4a-b**, **5a-b**, **6a-b** and **7a-b** in comparison with prototype **I** and kojic acid

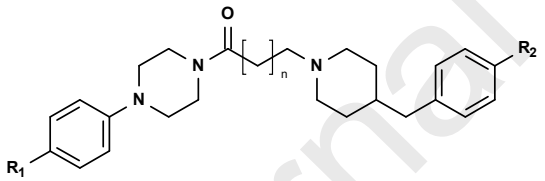

Compound	n	R_1	R_2	IC_{50} (µM)[a]
4a	0	H	H	80.86 ± 5.21
4b	0	OH	H	3.80 ± 0.48
5a	0	H	F	9.60 ± 0.08
5b	0	OH	F	4.49 ± 0.13
6a	1	H	H	57.50 ± 10.4
6b	1	OH	H	4.03 ± 1.18
7a	1	H	F	23.36 ± 2.16
7b	1	OH	F	6.06 ± 0.53
I	-	-	-	7.56 ± 1.90
kojic acid	-	-	-	17.76±0.18

[a]All compounds were examined in a set of experiments performed in three replicates; IC_{50} values represent the concentration that caused 50% enzyme activity loss.

fold more potent than corresponding unsubstituted analogue **4a**. Moreover, a dramatical improvement of activity (about 20-fold) resulted from the introduction of the hydroxyl substituent as observed by the comparison of IC_{50} values measured for unsubstitued compound **4a** (R_1=H, IC_{50} = 80.86 µM) respect to analogue **4b** (R_1=OH, IC_{50} = 3.80 µM). Interestingly, **4b** was the best active inhibitor of the series, which proved to be about 5-fold more potent than reference compound kojic acid. Further modifications were carried out for the carbon spacer linking the benzylpiperidine moiety with 4-phenyl-piperazine one. SAR consideration suggested that the lengthening of the carbon linker does not significantly affect the inhibitory effects as found for compound **4b** when compared with **6b** (IC_{50} = 4.03 µM), which bears an additional methylene bridge (n=1). In a similar way the compound **5b** (IC_{50} = 4.49 µM) and **7b** (IC_{50} = 6.6 µM) were equipotent as TyM inhibitors. Therefore, we can assume that the presence of a 4-hydroxylphenylpiperazine and/or 4-fluorobenzylpiperidine motif enable the better TYR inhibition.

To start with our studies on this new class of TYRIs we elected compound **4b** as prototype. Therefore, this compound was profiled to understand the mechanism of inhibition of TYR activity as well as to analyse additional biological properties. First of all, compound **4b** was selected for further kinetic studies; thereby its inhibitory activity on diphenolase activity was measured as a function of increasing concentration of L-DOPA. The obtained results are presented using Lineweaver-Burk double reciprocal plots (see Figure 4).

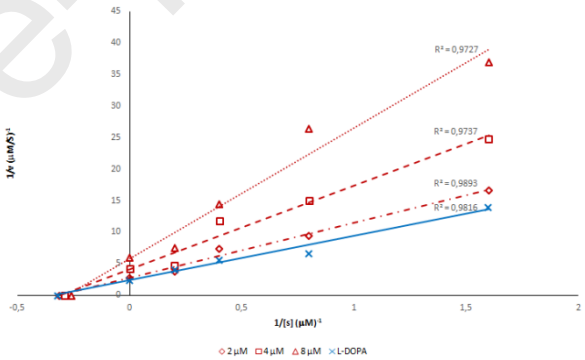

Figure 4. Lineweaver-Burk plots for the inhibition of tyrosinase respect to L-DOPA as substrate in the presence of **4b**.

As shown in Figure 4 the plots of 1/V versus 1/[S] gave straight lines with different slopes intersecting on the horizontal axis. These data suggested that compound **4b** acts as non-competitive inhibitor since it is able to bind with equal affinity to the free enzyme as well as to the enzyme-substrate complex. As a consequence, the increase of **4b** concentration entails the decrease of V_m value, while K_m value remains unchanged.

Then, the biosafety of the promising compound **4b** was further evaluated. Cells were treated with compound **4b** at concentrations ranging from 1 to 100 µM for 48 h at 37 °C and their potential cytotoxic effect on HeLa cells was determined using the MTT test. Compound **4b** exhibited no cytotoxic effect until 10 µM (Figure 5).

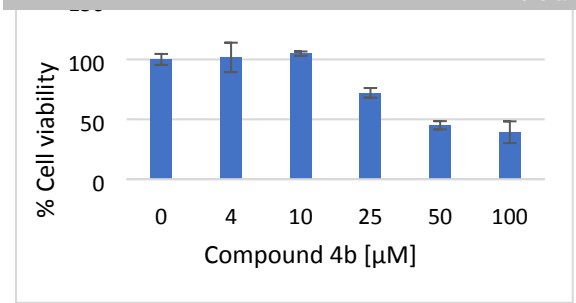

Figure 5. Effect of compound **4b** on HeLa cell viability. Data represent the mean (±standard deviation) of three independent experiments.

Moreover, the antioxidant activity of the compound **4b** was assessed by its ability to scavenge the ABTS radical and the result is represented as EC_{50} value in Table 2. Interestingly, the compound **4b** was found to possess an ability to quench ABTS radical and displayed a scavenging activity comparable to that of the positive control Trolox. [21]

Table 2. Antioxidant activity of compound **4b**.

Compound	EC_{50} (µM)[a]
4b	18.1 ± 0.4
Trolox[b]	13.0 ± 1.1

[a]Data represent the mean (± standard deviation, SD) of three independent experiments. [b]Positive control

Finally, to hypothesize the binding mode of this new series of inhibitors within TyM active site, docking studies were performed by using Gold software employing the crystal structure of TyM from *A. bisporus* (PDB 2Y9X). Figure 6A displays the plausible binding mode for the most active compounds **4b** within catalytic cavity. For a comparative purpose we carried out also the docking simulations for inhibitor **4a** (see Figure 6B), that was about 20-fold less active when compared with **4b** (see Table 1).

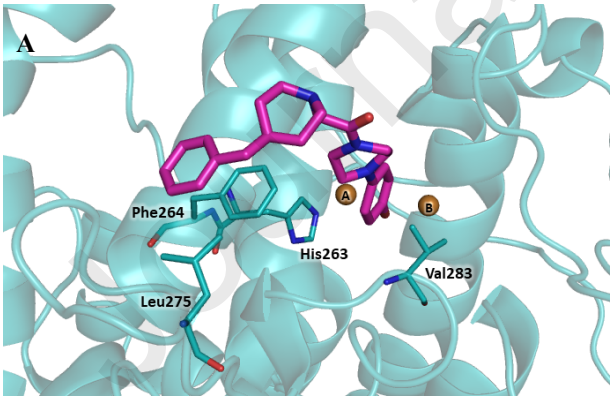

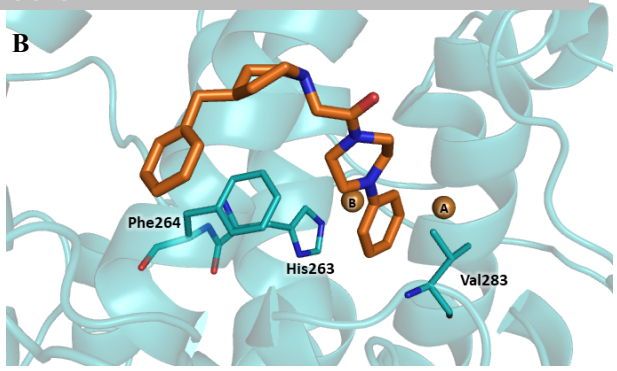

Figure 6. Plausible binding mode of compound **4b** (A) (magenta stick) and compound **4a** (B) (orange stick) that were docked into the TyM catalytic site from *A. bisporus* (PDB 2Y9X). Copper ions are represented by brown spheres. The residues of the binding site involved in the interaction with the ligand are highlighted as cyan sticks. All structures were generated by PyMOL (https://pymol.org).

Throughout the visual inspection of the hypothetical interactions, we found that **4a** and **4b** display a marked similarity in binding modes and share the network of contacts with residues paving the hydrophobic wall of cavity (*e.g.* Val283 and Phe264); furthermore, in both structures the 4-phenyl ring engages π-π interactions with His263. Thus, we hypothesize that the higher potency of inhibitor **4b** might be explained by the presence of a hydroxylphenyl substituent that is positioned close to the copper ions in the deep part of catalytic pocket similarly to 4-fluorobenzyl fragment for derivative **I** as well as other TyIs.[22-25]

3. Conclusions

In this work, we have investigated the TyM inhibitory effects of eight new molecules inspired by previously active inhibitor **I** having a benzylpiperidine crucial fragment. It is interesting to note that all obtained compounds inhibited tyrosinase from *Agaricus bisporus* (TyM*)* at micromolar concentration. Especially, compound **4b** displays IC_{50} value of 3.80 µM thus proving to be more active than kojic acid and our prototype **I**, that were used as reference compounds in the same test. Kinetics studies revealed that compound **4b** is a non-competitive diphenolase inhibitor of TyM and its binding mode was hypothesized by molecular docking studies. In addition, compound **4b** shows antioxidant effects and biosafety.

The most interesting outcome of this research was to find a new class of TYRIs from synthetic source providing antioxidant effects useful as dual effective agents.

4. Experimental section

4.1. Chemistry

All reagents were used without further purification and bought from common commercial suppliers. Microwave-assisted reactions were carried out in a Focused Microwawe TM Synthesis System, Model Discover (CEM Technology Ltd Buckingham, UK). Melting points were determined on a Buchi B-545 apparatus (BUCHI Labortechnik AG Flawil, Switzerland) and are uncorrected. Combustion analysis (C, H, N) was carried out on a Carlo Erba Model 1106-Elemental Analyzer to determine the purity of synthesized compounds; the results confirmed a ≥95% purity. Merck Silica Gel 60 F254 plates were used for analytical TLC (Merck KGaA, Darmstadt, Germany). Flash

Chr... (Biotage AB Uppsala, Sweden). ^{1}H NMR and ^{13}C NMR spectra were measured in dimethylsulfoxide-d6 (DMSO-d_6) with a Varian Gemini 500 spectrometer (Varian Inc. Palo Alto, California USA); chemical shifts are expressed in δ (ppm) and coupling constants (J) in hertz. All exchangeable protons were confirmed by addition of D_2O. R_f values were determined on TLC plates using a mixture of DCM/MeOH (96/4) as eluent. None of the studied compounds demonstrated PAINS alerts determined by SwissADME server (www.swissadme.ch).

4.1.1. *General procedure to synthesize 2-chloro-1-(4-phenylpiperazin-1-yl)ethanones (2a, 2b) and 3-chloro-1-(4-phenylpiperazin-1-yl)propan-1-ones (3a, 3b)*

To a solution of phenylpiperazine (1a or 1b) (3 mmol) in dry DCM (4 ml) the appropriate chloroacetyl chloride (3 mmol, 233.2 µl) or chloropropanoyl chloride (3 mmol, 286.4 µl) was added slowly (0°C). Then, the reaction mixture was stirred at room temperature for 1 hr. A saturated solution of $NaHCO_3$ (5 mL) was added to quench the reaction. The mixture was extracted with DCM twice, dried over Na_2SO_4 and the solvent was removed under vacuum. The desired compounds **2a-b** e **3a-b** were obtained as powder by treatment with EtOH and Et_2O. For these intermediates registered CAS numbers have been already assigned. For compound **3b** the synthetic procedure, chemical properties and structural characterization are not available in literature.

4.1.1.1. 2-Chloro-1-(4-phenylpiperazin-1-yl)ethanone (2a) CAS 1476139-8

Yield: 50%; white powder; M.p.: 75-76°C. 1H-NMR (DMSO-d_6): (δ) 3.10-3.50 (m, 8H, CH_2), 4.42 (s, 2H, CH_2-Cl), 6.69-7.25 (m, 5H, ArH). Anal. for ($C_{12}H_{15}ClN_2O$): C 60.38, H 6.33, N 11.73. Found: C 60.00, H 6.52, N 11.70.

4.1.1.2. 2-Chloro-1-[4-(4-hydroxyphenyl)piperazin-1-yl]ethanone (2b) CAS 75049-21-7

Yield: 30%; white powder; M.p.: 162-163°C. ^{1}H-NMR (DMSO-d_6): (δ) 2.91-3.56 (m, 8H, CH_2), 4.40 (s, 2H, CH_2-Cl), 6.64 (d, *J=8.2*, 2H, ArH), 6.78-6.9 (d, *J=8.2*, 2H, ArH), 8.88 (bs, 1H, OH). Anal. for ($C_{12}H_{15}ClN_2O_2$): C 56.59, H 5.94, N 11.00. Found: C 56.66, H 5.70, N 11.22.

4.1.1.3. 3-Chloro-1-(4-phenylpiperazin-1-yl)propan-1-one (3a) CAS 2392-47-4

Yield: 88%; white powder; M.p.: 84-85°C. ^{1}H-NMR (DMSO-d_6): (δ) 2.84-2.91 (m, 2H, CH_2Cl), 3.33-3.12 (m, 8H CH_2), 3.76-3.82 (m, 2H, CH_2-CO), 6.78-7.25 (m, 5H, ArH). Anal. for ($C_{13}H_{17}ClN_2O$): C 61.78, H 6.78, N 11.08. Found: C 61.89, H 6.40, N 11.30.

4.1.1.4. 3-Chloro-1-[4-(4-hydroxyphenyl)piperazin-1-yl]propan-1-one (3b) CAS 1183257-03-5

Yield: 97%; white powder; M.p.: 174-175°C. ^{1}H-NMR (DMSO-d_6): (δ) 2.83-2.89 (m, 2H, CH_2Cl), 2.89-3.56 (m, 8H CH_2), 3.77-3.81 (m, 2H, CH_2-CO), 6.65 (d, *J= 8.8,* 2H, ArH), 6.80 (d, *J= 8.8,* 2H, ArH), 8.89 (bs, 1H, OH). Anal. for ($C_{13}H_{17}ClN_2O_2$): C 58.10, H 6.38, N 10.42. Found: C 58.32, H 6.50, N 10.20.

4.1.2. *General procedure to synthesize 2-(4-benzyl-1-piperidyl)-1-(4-phenylpiperazin-1-yl)ethanones ... 4-phenylpiperazin-1-yl)propan-1-ones (6a, 6b, 7a, 7b)*

To a solution of 2-chloro-1-(4-phenylpiperazin-1-yl)ethanones (**2a-b**) or 3-chloro-1-(4-phenylpiperazin-1-yl)propan-1-ones (**3a-b**) (1.0 mmol) in DMF (1 mL) the appropriate amine derivative (1.5 mmol) and K_2CO_3 (0.5 mmol) were added. The reaction was heated using microwave irradiation for 15 min at 100 °C and then was quenched with water (5 mL) and a saturated solution of $NaHCO_3$ (5mL). The aqueous layer was extracted with EtOAc (3x10 mL) and obtained organic phases were washed with brine, filtered, concentrated and finally purified by flash chromatography (DCM/MeOH, 96:4) and crystallized with Et_2O and EtOH to afford desired pure compounds **4a, 4b, 5a, 5b, 6a, 6b, 7a,** and **7b**. For compounds **4a** and **6a** registered CAS numbers have been already assigned; however, their synthetic procedure, chemical properties and structural characterization are not available in literature. Therefore, we synthesized all designed compounds **4a, 4b, 5a, 5b, 6a, 6b, 7a,** and **7b** and their chemical characterization is reported below.

4.1.2.1. 2-(4-Benzyl-1-piperidyl)-1-(4-phenylpiperazin-1-yl)ethanone (4a) CAS 946939-23-7

Yield: 30%; white powder; M.p.: 95-96°C; R_f = 0.34. ^{1}H-NMR (DMSO-d_6): (δ) 1.14-3.67 (m, 2H, 21H), 6.77-7.25 (m, 10H, ArH). Anal. for ($C_{24}H_{31}N_3O$): C 76.36, H 8.28, N 11.13. Found: C 76.48 H 8.07 N 11.44.

4.1.2.2. 2-(4-Benzyl-1-piperidyl)-1-[4-(4-hydroxyphenyl)piperazin-1-yl]ethanone (4b)

Yield: 89%; white powder; M.p.: 183-184°C; R_f = 0.13. ^{1}H-NMR (DMSO-d_6): (δ) 1.12-3.65 (m, 20H), 6.65 (d, *J=8.7*, 2H, ArH), 6.79 (d, *J=8.7*, 2H, ArH), 7.12-7.27 (m, 5H, ArH), 8.83 (bs, 1H, OH). ^{13}C-NMR (DMSO-d_6): 31.81, 37.09, 41.31, 42.36, 45.32, 50.33, 50.99, 53.09, 61.43, 115.53, 118.40, 125.74, 128.13, 128.99, 140.36, 144.02, 151.35, 167.66. Anal. for $C_{24}H_{31}N_3O_2$: C 73.25, H 7.94, N 10.68. Found: C 73.26, H 7.93, N 10.69.

4.1.2.3. 2-[4-[(4-Fluorophenyl)methyl]-1-piperidyl]-1-(4-phenylpiperazin-1-yl)ethanone (5a)

Yield: 20%; pale yellow powder; M.p.: 95-97°C; R_f = 0.34. ^{1}H-NMR (DMSO-d_6): (δ) 1.12-3.67 (m, 21H), 6.79-7.22 (m, 9H, ArH). Anal. for ($C_{24}H_{30}FN_3O$): C 72.88, H 7.65, N 10.62. Found: C 72.69 H 7.44 N 10.84.

4.1.2.4. 2-[4-[(4-Fluorophenyl)methyl]-1-piperidyl]-1-[4-(4-hydroxyphenyl)piperazin-1-yl]ethanone (5b)

Yield: 66%; pale yellow powder; M.p.: 184-185°C; R_f = 0.13. ^{1}H-NMR (DMSO-d_6): (δ) 1.13-3.68 (m, 21H), 6.64 (d, *J=8.7*, 2H, ArH), 6.81 (d, *J=8.7*, 2H, ArH), 7.07-7.20 (m, 4H, ArH), 8.89 (bs, 1H, OH). Anal. for ($C_{24}H_{30}FN_3O_2$): C 70.05, H 7.35, N 10.21. Found: C 70.16, H 7.24, N 10.29.

4.1.2.5. 3-(4-Benzyl-1-piperidyl)-1-(4-phenylpiperazin-1-yl)propan-1-one (6a) CAS 1905697-95-1

Yield: 36%; white powder; M.p.: 67-68°C; R_f = 0.10. ^{1}H-NMR (DMSO-d_6): (δ) 1.08-3.56 (m, 23H), 6.76-7.27 (m, 10H, ArH). ^{13}C-NMR (DMSO-d_6): 31.81, 37.09, 40.88, 44.80, 45.32, 50.33, 50.99, 53.09, 61.43, 115.82, 119.37, 125.73, 128.18, 128.98, 140.34, 144.02, 150.83, 169.76. Anal. for ($C_{25}H_{33}N_3O$): C 76.69, H 8.49, N 10.73. Found: C 76.78, H 8.28, N 10.55.

4.1. [illegible] AZZ hydroxyphenyl)piperazin-1-yl]propan-1-one (6b)

Yield: 90%; white powder; M.p.: 158-159°C; R_f = 0.02. ^{1}H-NMR (DMSO-d_6): (δ) 1.13-3.53 (m, 23H), 6.64 (d, *J=8.8*, 2H, ArH), 6.79 (d, *J=8.8*, 2H, ArH), 7.06-7.18 (m, 5H, ArH), 8.89 (bs, 1H, OH). ^{13}C-NMR (DMSO-d_6): 31.81, 37.09, 40.27, 42.43, 45.32, 50.33, 50.99, 53.09, 61.43, 115.53, 118.40, 125.74, 128.13, 128.99, 140.36, 144.41, 151.78, 170.23. Anal. for ($C_{25}H_{33}N_3O_2$): C 73.68, H 8.16, N 10.31. Found: C 73.59, H 8.05, N 10.40.

4.1.2.7. 3-[4-[(4-Fluorophenyl)methyl]-1-piperidyl]-1-(4-phenylpiperazin-1-yl)propan-1-one (7a)

Yield: 20%; white powder; M.p.: 206-207°C; R_f = 0.07. ^{1}H-NMR (DMSO-d_6): (δ) 1.13-3.56 (m, 23H), 6.62-7.20 (m, 8H, ArH). Anal. for ($C_{25}H_{32}FN_3O$): C 73.32, H 7.88 N 10.26. Found: C 73.54, H 7.60, N 10.35.

4.1.2.8. 3-[4-[(4-Fluorophenyl)methyl]-1-piperidyl]-1-[4-(4-hydroxyphenyl)piperazin-1-yl]propan-1-one (7b)

Yield: 79%; white powder; M.p.: 170-171°C; R_f = 0.02. ^{1}H-NMR (DMSO-d_6): (δ) 1.13-3.53 (m, 23H), 6.63 (d, *J=8.8,* 2H, ArH), 6.77 (d, *J=8.8,* 2H, ArH), 7.06-7.18 (m, 4H, ArH), 8.89 (bs, 1H, OH). Anal. for ($C_{25}H_{32}FN_3O_2$): C 70.56, H 7.58, N 9.87. Found: C 70.44. H 7.46, N 9.68.

4.2. Mushroom tyrosinase inhibition assay

Tyrosinase inhibition was assayed according to the method of Masamoto, [26] with minor modifications. [27] Briefly, aliquots (0.05 mL) of sample at various concentrations (5-300 μM) were mixed with 0.5 mL of L-DOPA solution (1.25 mM), 0.9 mL of sodium acetate buffer solution (0.05 M, pH 6.8) and preincubated at 25°C for 10 min. Then 0.05 mL of an aqueous solution of mushroom tyrosinase (333 U/mL) was added last to the mixture. The linear increase in absorbance (Abs) at 475 nm was measured in the reaction mixture up to 5 minutes. The inhibitory activity of samples is expressed as inhibition percentage. The concentrations leading to 50% activity loss (IC_{50}) were also calculated by interpolation of the dose-response curves. Kojic acid [5-hydroxy-2-(hydroxymethyl)-4H-pyran-4-one], a fungal secondary metabolite used as skin whitening agent, was employed as a positive standard (8-35 μM).

4.3. Kinetic analysis of the tyrosinase inhibition

The reaction mixture consisted of four different concentrations of L-DOPA (0.6–5 mM), the substrate, and mushroom tyrosinase in acetate buffer (0.05 M, pH 6.8). Three different concentrations of compound **4b** (2, 4, and 8 μM) were added to the reaction mixture. The Michaelis-Menten constant (Km) and maximal velocity (Vmax) of tyrosinase were determined by Lineweaver-Burk plots.

4.4. Docking Studies

The crystal structure of TyM in complex with inhibitor tropolone was retrieved from the RCSB Protein Data Bank (PDB code 2Y9X).[9] The ligand and water molecules were removed, and hydrogens were added to the protein by means of Discovery Studio 2.5.5 (Discovery Studio 2.5.5 Accelrys http://www.accelrys.com., San Diego, CA, 2009). Ligands structures were constructed by VEGAZZ suite and optimized by following a conjugate gradient program. [28] Docking studies were performed by using Gold software version 5.7.1 employing the same protocol as reported in our previous papers [20] with slight modifications. In particular the pyramidal nitrogen and amide bonds were allowed to rotate, and no constraints were applied. ChemPLP was chosen as fitness score. The best scored pose for each ligand was chosen for the analysis and representation.

4.5. Cell viability assay

The human cervical carcinoma HeLa cell line was grown in DMEM medium supplemented with 10% fetal bovine serum (FBS), 2 mM L-Glutamine, penicillin (100U/mL) and streptomycin (100 μg/mL) at 37 °C in 5% CO_2. Cell Growth was evaluated culturing 3 × 10^4/mL Hela cells in 96 well plates. Cell viability was detected by the colorimetric 3-(4,5-dimethylthiazol-2-yl)-2,5-diphenyltetrazolium bromide (MTT) assay. This is a colorimetric assay for measuring the activity of mitochondrial enzymes in living cells that convert MTT into purple formazan crystals. Briefly, cells were seeded in a 96-well plate and incubated with samples at concentration ranging from 4 to 100 μM for 48 h. Since DMSO was used as solvent for compounds, cell viability was evaluated also in the presence of DMSO alone, as solvent control. After incubation time, MTT solution (final concentration 0.5 mg/mL) was then added to each well and incubated for 3 h at 37 °C. The cells were lysed with 100 μL of DMSO and the optical density was measured at 560 nm with an auto microplate reader (Multiskan FC – Thermo Scientific). The mean value and standard deviation (SD) were calculated from triplicate experiments.

4.6. Antioxidant Activity

The total free radical-scavenging capacity of compound was determined by ABTS [2,2'-azinobis-(3-ethylbenzothiazoline-6-sulfonic acid)] method using 6-hydroxy-2,5,7,8-tetramethylchromane-2-carboxylic acid (Trolox) as standard, as previously described. [29] The $ABTS^{\bullet+}$ method is based on the capacity of an antioxidant to scavenge the free $ABTS^{\bullet+}$. $ABTS^{\bullet+}$ reagent was produced by reacting 7 mM ABTS with 2.45 mM potassium persulfate (final concentration) in aqueous solution. The mixture was kept in the dark, at room temperature, for 24 h. The concentration of the blue-green $ABTS^{\bullet+}$ solution was adjusted to an absorbance of 0.700 ± 0.02 at 734 nm. The samples of the compound were added to $ABTS^{\bullet+}$ solution and incubated in the dark at room temperature for 1 min. Afterwards the decrease in A_{734} was calculated and referred to the trolox standard curve. Antioxidant activity was expressed as concentration of the compound to give a 50% reduction in the original absorbance (EC_{50}).

Acknowledgements

This work was supported by the MIUR - "Finanziamento delle Attività Base di Ricerca" FFABR funding 2017.

References

1. Sánchez-Ferrer A, Rodríguez-López JN, García-Cánovas F, García-Carmona F. Tyrosinase: a comprehensive review of its mechanism. *Biochim Biophys Acta.* 1995**;** 1247: 1-11.

2. Pillaiyar T, Namasivayam V, Manickam M, Jung SH. Inhibitors of Melanogenesis: An Updated Review. *J Med Chem.* 2018**;** 61: 7395-7418.

3. Manandhar B, Wagle A, Seong SH, Paudel P, Kim HR, Jung HA, Choi JS. Phlorotannins with Potential Anti-tyrosinase and Antioxidant Activity Isolated from the Marine Seaweed. *Antioxidants (Basel).* 2019**;** 8. doi: 10.3390/antiox8080240

4. Zo... *Mol Inform.* 2020; 39:e1900034. doi: 10.1002/minf.201900034.
F, Garcia-Canovas F, Saboury AA. A comprehensive review on tyrosinase inhibitors. *J Enzyme Inhib Med Chem.* 2019**;** 34: 279-309.
5. Burdock GA, Soni MG, Carabin IG. Evaluation of health aspects of kojic acid in food. *Regul Toxicol Pharmacol.* 2001**;** 33: 80-101.
6. Bentley R. From miso, saké and shoyu to cosmetics: a century of science for kojic acid. *Nat Prod Rep.* 2006**;** 23: 1046-1062.
7. Lajis AF, Hamid M, Ariff AB. Depigmenting effect of Kojic acid esters in hyperpigmented B16F1 melanoma cells. *J Biomed Biotechnol.* 2012**;** 2012: 952452. doi: 10.1155/2012/952452
8. Kim H, Choi J, Cho JK, Kim SY, Lee YS. Solid-phase synthesis of kojic acid-tripeptides and their tyrosinase inhibitory activity, storage stability, and toxicity. *Bioorg Med Chem Lett.* 2004**;** 14: 2843-2846.
9. Ismaya WT, Rozeboom HJ, Weijn A, Mes JJ, Fusetti F, Wichers HJ, Dijkstra BW. Crystal structure of Agaricus bisporus mushroom tyrosinase: identity of the tetramer subunits and interaction with tropolone. *Biochemistry.* 2011**;** 50: 5477-5486.
10. Kubo I, Kinst-Hori I, Chaudhuri SK, Kubo Y, Sánchez Y, Ogura T. Flavonols from Heterotheca inuloides: tyrosinase inhibitory activity and structural criteria. *Bioorg Med Chem.* 2000**;** 8: 1749-1755.
11. Xie LP, Chen QX, Huang H, Wang HZ, Zhang RQ. Inhibitory effects of some flavonoids on the activity of mushroom tyrosinase. *Biochemistry (Mosc).* 2003**;** 68: 487-491.
12. No JK, Soung DY, Kim YJ, Shim KH, Jun YS, Rhee SH, Yokozawa T, Chung HY. Inhibition of tyrosinase by green tea components. *Life Sci.* 1999**;** 65: PL241-246.
13. Pintus F, Matos MJ, Vilar S, Hripcsak G, Varela C, Uriarte E, Santana L, Borges F, Medda R, Di Petrillo A, Era B, Fais A. New insights into highly potent tyrosinase inhibitors based on 3-heteroarylcoumarins: Anti-melanogenesis and antioxidant activities, and computational molecular modeling studies. *Bioorg Med Chem.* 2017**;** 25: 1687-1695.
14. Ferro S, Certo G, De Luca L, Germanò MP, Rapisarda A, Gitto R. Searching for indole derivatives as potential mushroom tyrosinase inhibitors. *J Enzyme Inhib Med Chem.* 2016**;** 31: 398-403.
15. Ferro S, Deri B, Germanò MP, Gitto R, Ielo L, Buemi MR, Certo G, Vittorio S, Rapisarda A, Pazy Y, Fishman A, De Luca L. Targeting Tyrosinase: Development and Structural Insights of Novel Inhibitors Bearing Arylpiperidine and Arylpiperazine Fragments. *J Med Chem.* 2018**;** 61: 3908-3917.
16. Ielo L, Deri B, Germanò MP, Vittorio S, Mirabile S, Gitto R, Rapisarda A, Ronsisvalle S, Floris S, Pazy Y, Fais A, Fishman A, De Luca L. Exploiting the 1-(4-fluorobenzyl)piperazine fragment for the development of novel tyrosinase inhibitors as anti-melanogenic agents: Design, synthesis, structural insights and biological profile. *Eur J Med Chem.* 2019**;** 178: 380-389.
17. Vittorio S, Seidel T, Germanò MP, Gitto R, Ielo L, Garon A, Rapisarda A, Pace V, Langer T, De Luca L. A Combination of Pharmacophore and Docking-
18. Gitto R, De Luca L, Ferro S, Scala A, Ronsisvalle S, Parenti C, Prezzavento O, Buemi MR, Chimirri A. From NMDA receptor antagonists to discovery of selective sigma(2) receptor ligands. *Bioorg Med Chem.* 2014**;** 22: 393-397.
19. Gitto R, De Luca L, Ferro S, Citraro R, De Sarro G, Costa L, Ciranna L, Chimirri A. Development of 3-substituted-1H-indole derivatives as NR2B/NMDA receptor antagonists. *Bioorg Med Chem.* 2009**;** 17: 1640-1647.
20. Ferro S, De Luca L, Germanò MP, Buemi MR, Ielo L, Certo G, Kanteev M, Fishman A, Rapisarda A, Gitto R. Chemical exploration of 4-(4-fluorobenzyl)piperidine fragment for the development of new tyrosinase inhibitors. *Eur J Med Chem.* 2017**;** 125: 992-1001.
21. Kumar A, Pintus F, Di Petrillo A, Medda R, Caria P, Matos MJ, Viña D, Pieroni E, Delogu F, Era B, Delogu GL, Fais A. Novel 2-pheynlbenzofuran derivatives as selective butyrylcholinesterase inhibitors for Alzheimer's disease. *Sci. Rep.* 2018**;** 8: 4424. doi: 10.1038/s41598-018-22747-2.
22. Nazir Y, Saeed A, Rafiq M, Afzal S, Ali A, Latif M, Zuegg J, Hussein WM, Fercher C, Barnard RT, Cooper MA, Blaskovich MAT, Ashraf Z, Ziora ZM1.Hydroxyl substituted benzoic acid/cinnamic acid derivatives: Tyrosinase inhibitory kinetics, anti-melanogenic activity and molecular docking studies. *Bioorg Med Chem Lett.* 2020; 30: 126722. doi: 10.1016/j.bmcl.2019.126722;
23. Sheng Z, Ge S, Xu X, Zhang Y, Wu P, Zhang K, Xu X, Li C, Zhao D, Tang X. Design, synthesis and evaluation of cinnamic acid ester derivatives as mushroom tyrosinase inhibitors. *Medchemcomm.* 2018; 9:853-861.
24. Radhakrishnan S, Shimmon R, Conn C, Baker A. Development of hydroxylated naphthylchalcones as polyphenol oxidase inhibitors: Synthesis, biochemistry and molecular docking studies. *Bioorg Chem.* 2015;63:116-22.
25. Tang J, Liu J, Wu F. Molecular docking studies and biological evaluation of 1,3,4-thiadiazole derivatives bearing Schiff base moieties as tyrosinase inhibitors. *Bioorg Chem*. 2016; 69:29-36.
26 Masamoto Y, Ando H, Murata Y, Shimoishi Y, Tada M, Takahata K. Mushroom tyrosinase inhibitory activity of esculetin isolated from seeds of Euphorbia lathyris L. *Biosci Biotechnol Biochem.* 2003**;** 67: 631-634.
27. Germanò MP, Cacciola F, Donato P, Dugo P, Certo G, D'Angelo V, Mondello L, Rapisarda A. Betula pendula leaves: polyphenolic characterization and potential innovative use in skin whitening products. *Fitoterapia.* 2012**;** 83: 877-882.
28. Pedretti A, Villa L, Vistoli G. VEGA - An open platform to develop chemo-bio-informatics applications, using plug-in architecture and script programming. *J Comput Aid Mol Des.* 2004**;** 18: 167-173.
29. Fais A, Kumar A, Medda R, Pintus F, Delogu F, Matos MJ, Era B, Delogu GL. Synthesis, molecular docking and cholinesterase inhibitory activity of hydroxylated 2-phenylbenzofuran derivatives. *Bioorg Chem.* 2019**;** 84: 302-308.